Available online at www.sciencedirect.com
SCIENCE DIRECT®
Archives of Biochemistry and Biophysics 431 (2004) 31–46
ABB
www.elsevier.com/locate/yabbi

Kidney ischemia–reperfusion regulates expression and distribution of tubulin subunits, β-actin and rho GTPases in proximal tubules

Annick Caron, Richard Raoul Desrosiers, Richard Béliveau*

Laboratoire de médecine moléculaire, Centre de cancérologie Charles Bruneau, Hôpital Ste-Justine, Université du Québec à Montréal, C.P. 8888, Succursale Centre-Ville, Montreal, Que., Canada, H3C 3P8

Received 11 May 2004, and in revised form 12 July 2004
Available online 27 August 2004

Abstract

Ischemic injury is characterized by a loss of cell polarity and a release of proximal tubule epithelial cells resulting from cytoskeletal reorganization. This study used a reversible unilateral renal ischemia–reperfusion model to investigate the expression and distribution of cytoskeletal components and Rho GTPases at protein and mRNA levels in proximal tubule fractions. Ischemia strongly increased β-actin and α-tubulin expressions that were predominantly found in nuclear fractions. Rho GTPases and caveolin-1 expression were upregulated by ischemia and were enriched mainly in Triton-soluble membranes. Rac1 expression was stimulated in the soluble fractions during reperfusion. Rho GTPases mRNA levels were similarly regulated by ischemia–reperfusion suggesting that changes in their expressions could occur at gene or mRNA levels. ERM protein expression and distribution were unaffected by ischemia–reperfusion. Together, these data show that renal ischemia–reperfusion induced expression and redistribution of actin and microtubule cytoskeleton components in addition to Rho GTPases in proximal tubules, suggesting that they participate in an adaptive response to cellular lesions.
© 2004 Published by Elsevier Inc.

Keywords: Ischemia; Reperfusion; Tubulin subunits; RhoGTPases; Caveolin-1; ERM

In adults, ischemia remains the leading cause of acute renal failure [1]. Thus, kidney injury caused by ischemia and reperfusion is a major focus for both fundamental and clinical research. The epithelial cells of proximal tubules are particularly sensitive to ischemic injury [2]. In vivo, ischemic acute renal failure has been shown to induce apical membrane disruption by a collapse of microvilli, leading to a loss of cell polarity in proximal tubules. In addition, renal ischemia reduces cell attachment that leads to renal tubular obstruction by released epithelial cells and vasoconstriction of afferent arterioles to glomeruli [3]. All these changes are accompanied, to some degree, by a reorganization of the actin cytoskeleton. In epithelial cells, the actin network is a major regulator of cell morphology [4]. Several studies used immunohistochemical techniques to demonstrate that kidney ischemia induced actin depolymerization and collapse, and that this occurs within 5 min of ischemia [5,6]. However, the mechanism by which ischemia–reperfusion regulates actin expression at the mRNA and protein levels remains unknown.

* Corresponding author. Fax: +1 514 987 0246.
E-mail addresses: oncomol@nobel.si.uqam.ca (R. Béliveau), annick.caron@videotron.ca (R. Béliveau).

0003-9861/$ - see front matter © 2004 Published by Elsevier Inc.
doi:10.1016/j.abb.2004.07.009

Ezrin, moesin, and radixin (ERM)[1] are members of a family of proteins that link the plasma membrane to the actin cytoskeleton and are a primary constituent of microvilli [7]. It has been demonstrated that renal anoxia and chemical ATP depletion in isolated proximal tubules results in ezrin-cytoskeleton dissociation, initiating microvillar breakdown [8,9]. However, the behavior of ERM proteins during kidney ischemia in living animals remains to be established.

Microtubules are filamentous structures composed of heterodimers of polymerized α- and β-tubulin subunits [10]. They are dynamic structures, continuously polymerizing and depolymerizing using a microtubule-organizing center with γ-tubulin as the starting point for polymerization [11]. This polymerization dynamic allows microtubules to adopt spatial arrangements that can change rapidly in response to cellular needs and, in some cases, to perform mechanical work [12]. Microtubules utilize the energy of GTP hydrolysis to fuel a unique polymerization mechanism [13]. It has been demonstrated immunohistochemically that 40 min of kidney ischemia induced a mild disruption of the microtubular network [14]. Heat shock proteins (HSP) are structurally and functionally related stress proteins induced by a variety of insults, including heat and ischemia [15]. Moreover, HSP73, a member of the HSP70 family, has been recently shown to colocalize with microtubules and with perinuclear and centrosomal tubulin following cardiac ischemia [16]. However, no study has yet studied the impact of reversible ischemia on the expression and distribution of different tubulin subunits.

Key regulators in cytoskeleton organization, the Rho GTPases are members of the Ras superfamily of GTP-binding proteins. Like all members of this superfamily, the Rho proteins function as molecular switches by cycling between an active state bound to GTP and an inactive state bound to GDP [17]. Rho family proteins are key players in the organization of the actin cytoskeleton into various structures [18]. In fibroblasts, Cdc42 induces filopodia formation [19], Rac1 induces membrane ruffling and lamellipodia [20], and RhoA induces stress fibers and focal adhesion [21]. Thus, Rho proteins are involved in the regulation of cell morphology, cell motility, cytokinesis, and apoptosis [22]. In addition, some GTPases such as Rac1 have been described to directly bind tubulin [23]. ATP depletion is known to cause Rho inactivation in renal epithelial cells, resulting in disruption of stress fibers [24,25]. RhoGDI (GDP dissociation inhibitor) is a regulator that binds to GDP-loaded Rho GTPases, preventing them from being converted to GTP-bound forms [26]. Recently, we reported that the phosphorylation state of certain Rho proteins regulates their interactions with RhoGDI and their extraction from membranes [27], suggesting new molecular mechanisms for the inhibition of Rho GTPases. Furthermore, we demonstrated that in cultured renal cell carcinoma (Caki-1), hypoxia (1% O_2) rapidly upregulated Rho protein expression and that RhoA was required for the accumulation of transcription factor, hypoxia inducible factor-1α (HIF-1α), essential to hypoxic response [28]. However, little information is available about the impact of ischemia–reperfusion injury on the expression and distribution of Rho GTPases in kidney.

Occludin is an extracellular component of tight junctions [29]. It has been reported that ATP depletion, anoxia, and ischemia resulted in an alteration of the functional integrity of tight junctions [30–32]. Tight junction protein affiliation with the apical actin cytoskeleton is crucial in regulating tight junction function. Regulation of tight junction permeability and occludin phosphorylation occur by a RhoA-dependent mechanism [33].

We previously reported that RhoA and Cdc42 are located in caveolae [34]. Caveolae are specialized membrane invaginations enriched in cholesterol and sphingolipids, which are also marked by the presence of caveolin-1 protein [35]. Furthermore, caveolae are thought to play an important role in signal transduction since several receptors for growth factors and signaling molecules are located in these structures [36]. The actin network seems to be directly involved in the organization of caveolae and Rho activation reorganizes caveolae localization [37]. In addition, the actin cytoskeleton and microtubules regulate the caveolar membrane traffic [38]. It has been demonstrated that acute proximal tubular injury damages caveolar/detergent resistant microdomain structures, characterized by deranged cholesterol distribution and caveolin release from plasma membranes [39].

There is considerable interest in understanding the cellular and biochemical mechanisms underlying ischemia–reperfusion injury. For the first time, this study used a reversible unilateral ischemia–reperfusion model to investigate the expression and distribution of the actin cytoskeletal, microtubular proteins and Rho GTPases at the mRNA and protein levels in living animals in proximal tubules during ischemic injury. Furthermore,

[1] *Abbreviations used:* ADF, actin depolymerizing factor; ATP, adenosine triphosphate; BSA, bovine serum albumin; cDNA, complementary deoxyribonucleic acid; DEPC, diethylpyrocarbonate; ERM, ezrin–moesin–radixin; F-actin, filamentous actin; G-actin, monomeric actin; GDP, guanosine diphosphate; GTP, guanosine triphosphate; HBSS, Hanks' balanced saline solution; HIF, hypoxia-inducible factor; Hepes, 4-(2-hydroxyethyl)-1-piperazineethanesulfonic acid; HSP, heat shock protein; Pak, p21 activated kinase; PP2A, protein phosphatase 2A; PVDF, polyvinylidene difluoride; RhoGDI, GDP dissociation inhibitor; RNA, ribonucleic acid; ROCK, Rho associated kinase; ROS, reactive oxygen species; RT-PCR, reverse transcription polymerase chain reaction; SDS, sodium dodecyl sulfate; SDS–PAGE, SDS–polyacrylamide gel electrophoresis; TBS-T, Tris-buffered saline Tween 20; Tris, tris(hydroxymethyl)aminomethane.

the expression of RhoGDI, which regulates Rho GTPases activity and subcellular localization, and of caveolin-1, which binds some Rho GTPases, has also been examined in kidney proximal tubules during acute ischemia–reperfusion.

Materials and methods

Materials

Male Sprague–Dawley rats (250–300 g body wt) were obtained from Charles River (Saint-Constant, Que.). Acepromazine and ketamine–HCl were from Ayerst Laboratories (Montréal, Que.) and xylazine–HCl was from Bayer (Etobicoke, Ont.). Rabbit polyclonal antibodies against Cdc42 (SC-87), RhoGDI (SC-360), and γ-tubulin (SC-10732), mouse monoclonal antibodies against RhoA (SC-418) and RhoB (SC-8048), goat polyclonal antibody against ezrin (SC-6407), against HSP70 (SC-1060), and donkey anti-goat horseradish peroxidase-conjugated antibody were purchased from Santa Cruz Biotechnology (Santa Cruz, CA). Rabbit polyclonal antibody against Caveolin (610059) and mouse monoclonal antibody against Rac1 (610651) were from BD Biosciences (Mississauga, Ont.). Mouse monoclonal antibodies against α-tubulin (CP06-100UG) and β-tubulin (CP007-100UG) were obtained from Oncogene (Uniondale, NY). Mouse monoclonal antibody against HIF-1α (NB 100-123) was purchased from Novus Biological (Littleton, CO). Rabbit polyclonal antibody against occludin (71–1500) was from Zymed Laboratories (San Francisco, CA). Donkey anti-rabbit and anti-mouse horseradish peroxidase-conjugated antibodies were from Jackson ImmunoResearch Laboratories (West Grove, PA). The Western Lightning chemiluminescence Reagent Plus (ECL) detection system was from NEN Life Science Products (Boston, MA). Mouse monoclonal antibody against β-actin (A5316) and against β-Cop (G2279) and diethylpyrocarbonate (DEPC) were from Sigma (St. Louis, MO). TriZol and Superscript One-Step RT-PCR with platinum *Taq* were from Invitrogen Life Technologies (Burlington, Ont.).

Ischemic and reperfusion treatments

Approval for rat experiments was obtained from CIPA (Comité institutionnel de bonnes pratiques animales en recherche, University of Québec at Montréal). Rats were anesthetized by subcutaneous injection of acepromazine (2.5 mg/kg) followed by intraperitoneal injection of ketamine–HCl (87 mg/kg) and xylazine–HCl (7 mg/kg). A ventral incision was made. The renal artery and vein of the left kidney were dissected and a non-traumatic Schwartz vascular clamp was placed around them to induce acute ischemia for 30 min. Ischemic kidneys were decapsulated to prevent collateral circulation to the superficial cortex through capsular vessels. To avoid reflow after ischemia, the clamps were left until kidneys were removed. In some cases, the clamp was removed and kidneys were reperfused for 60 min. The animals were placed on a heating pad to maintain a constant body temperature (37 °C). The sham groups were anesthetized and ventrally operated for 30 or 90 min. Rats were sacrificed by lethal exposure to carbon dioxide followed by decapitation. Kidneys, the left treated, were quickly removed and placed in ice-cold 0.85% NaCl solution. Experiments were done with kidneys pooled from six rats per group.

Evaluation of renal failure by creatinine levels

Creatinine levels were measured using the manufacturer's directions. Briefly, 300 μL serum was mixed with an alkaline picrate solution. Samples were then incubated at room temperature for 10 min. Measurements were done with a spectrophotometer at a wavelength of 500 nm. To remove any interference, 100 μL of a mixture of sulfuric and acetic acid was added to samples that were then incubated for another 5 min and read again at 500 nm. Serum creatinine levels were calculated as (mg/L) for each animal using a creatinine standard.

Isolation of proximal tubules

To isolate proximal tubules, minced kidney cortex was homogenized with a Dounce homogenizer (No. 7) in Hanks' balanced saline solution (HBSS) (1 mM $CaCl_2$, 5 mM KCl, 0.4 mM KH_2PO_4, 0.5 mM $MgCl_2 \cdot 6H_2O$, 0.5 mM $MgSO_4 \cdot 7H_2O$, 137 mM NaCl, 4 mM $NaHCO_3$, 0.3 mM Na_2HPO_4, and 6 mM D-glucose) at pH 7.4 and then collected on 103 μm Nylon mesh [40]. Tubules were resuspended in 250 mM sucrose, 10 mM Hepes–Tris, pH 7.4, and lysed with a Potter–Elvehjem motorized homogenizer followed by homogenization with a Polytron. Purity of isolated proximal tubules was confirmed by microscopic examination. To further validate proximal tubule preparations, alkaline phosphatase activity was assayed and its specific activity in proximal tubules was enriched 5-fold (data not shown) compared to cortex homogenates, in all preparations.

Biochemical fractionation of proximal tubules

Lysed proximal tubules were centrifuged at 3000*g* for 10 min at 4 °C to separate nuclei and unbroken cells from post-nuclear supernatants. These supernatants were then centrifuged at 100,000*g* for 1 h at 4 °C in order to separate crude membranes (pellets) from soluble fractions. Crude membranes were resuspended in 20 mM Hepes–Tris, pH 7.4. To prepare nuclear fractions, pellets obtained after the first centrifugation at 3000*g* were

incubated in a solution containing 250 mM sucrose, 10 mM Hepes–Tris, pH 7.4, and 0.2% (w/v) Triton X-100 for 10 min at room temperature and then centrifuged at 3000*g* for 10 min at 4 °C. Pellets contained the nuclear fractions. Proximal tubule homogenates, soluble fractions, crude membranes, and nuclear fractions were kept at −80 °C.

Solubilization of crude membranes in Triton X-100

Crude membranes (40 μg of protein) were incubated in 30 μL of 20 mM Hepes–Tris, pH 7.0, with 2% (w/v) Triton X-100 for 60 min at 37 or 4 °C. In some experiments, 150 mM KCl was added to the incubation buffer. After the incubation, membranes were centrifuged at 40,000*g* for 30 min at 4 °C to separate Triton-soluble membranes in supernatants from Triton-insoluble membranes in pellets as described previously [41].

Gel electrophoresis and immunoblotting

Proteins were quantified using the bicinchoninic acid micro-assay using a kit from Pierce (Rockford, Illinois) [42]. Proximal tubule fractions were incubated in sample buffer composed of 62.5 mM Tris–HCl, pH 6.8, 10% (v/v) glycerol, 5% (v/v) β-mercaptoethanol, 2% (w/v) SDS, and 0.00625% (w/v) bromophenol blue. Samples were heated at 100 °C for 3 min and then loaded onto polyacrylamide gels. SDS–PAGE was carried out according to Laemmli [43] at a constant 100 V. Proximal tubule proteins were transferred electrophoretically onto 0.45 μm pore diameter polyvinylidene difluoride (PVDF) membranes (Roche Molecular Biochemicals, Que., Canada) using a MilliBlot Graphite Electroblotter I apparatus (Millipore, Bedford, MA). The transfer buffer contained 96 mM glycine, 10 mM Tris, and 10% (v/v) methanol. Protein transfer was carried out for 1.5 h at a constant current of 1 mA/cm^2. Hydrophobic or non-specific sites were blocked with 5% (w/v) powdered skim milk in Tris-buffered saline (50 mM Tris and 137 mM NaCl) containing 0.3% (v/v) Tween 20 (TBS-T) for 1 h at room temperature. Membranes were washed three times for 15 min in TBS-T. PVDF membranes were incubated with antibodies in TBS-T containing 3% (w/v) bovine serum albumin (BSA) and 0.01% (w/v) NaN_3 overnight at 4 °C. Membranes were washed three times for 15 min and incubated for 1 h at room temperature with peroxidase-conjugated donkey anti-mouse IgG or donkey anti-rabbit IgG (1:2500) in TBS-T containing 5% (w/v) milk powder. PVDF membranes were washed three times for 15 min and localization of immunoreactive proteins with ECL Plus was performed as described previously [44]. Blots were exposed to Fuji films and autoradiograms were scanned with a Personal Densitometer (Molecular Dynamics, Sunnyvale, CA).

RNA isolation and RT-PCR

Proximal tubule isolation for RNA extraction was performed as described above with the exception that all solutions contained 0.1% diethylpyrocarbonate (DEPC) to inhibit RNases. Total RNA from proximal tubules was extracted with TriZol reagent using the manufacturer's directions and quantified by the OD_{260}. Reverse transcription, using SuperScript II RNAse H-Reverse Transcriptase, was done at 50 °C for 30 min with 1 μg RNA from proximal tubules. cDNA was amplified using Superscript One-Step RT-PCR with Platinum *Taq* from Invitrogen Life Technologies (Burlington, Ont.). The PCR primers used for β-actin, α-tubulin, β-tubulin, RhoA, RhoB, Rac1, Cdc42, and RhoGDI cDNA amplification and number of cycles done are listed in Table 1 and were derived from rat sequences (GenBank). Samples had a initial denaturation at 94 °C for 2 min and then amplified with the following parameters: denaturation at 94 °C for 30 s, annealing between 57.4 and 59.6 °C for 30 s, and elongation at 72 °C for 30 s. Samples had a final elongation at 72 °C for 10 min. cDNA fragments were analyzed on 1.8% agarose gels and then stained with ethidium bromide.

Statistical analysis

The results are expressed as means ± SEM of two experiments done in duplicate and analyzed with Student's *t* test. In the figures, only significant differences between treated kidneys and their corresponding sham kidneys are indicated.

Results

Serum creatinine levels as indicator of acute renal failure during ischemia–reperfusion

The hallmark of acute renal failure is a decreased glomerular filtration rate [3]. This diminution was assessed by measuring serum creatinine levels. During ischemia, creatinine levels were 1.3-fold higher compared to sham-operated controls ($p < 0.001$). During reperfusion, creatinine levels increased by 2.6-fold ($p < 0.001$) compared to controls (Table 2). Importantly, these data demonstrate that our reversible unilateral ischemia–reperfusion model in rats stimulated serum creatinine levels, indicating that renal failure occurred during treatments.

Ischemia–reperfusion induces β-actin expression and its release from membranes in proximal tubules

Proximal tubules were specifically chosen for this study due to their sensitivity to the well-documented cytoskeleton disruption caused by ischemic injury

Table 1
Sequences of oligonucleotides used as primers for RT-PCR assays

Target	Sequence	Hybridization temperature (°C)	Number of cycles	Product size (bp)
β-Actin fw	5′-GGCACCACACTTTCTACAATGAG-3′	57.2	25	178
β-Actin bw	5′-AGGCATACAGGGACAACACAGC-3′			
α-Tubulin fw	5′-GCCATTGCCACCATCAAGAC-3′	58.3	25	321
α-Tubulin bw	5′-CACACCAACCTCCTCATAATCCTTC-3′			
β-Tubulin fw	5′-TCACCTTCATCGGAAACAGCAC-3′	58.1	30	324
β-Tubulin bw	5′-CAGAGGCAGCAGAAAGAAACAAAG-3′			
RhoA fw	5′-CAGGTAGAGTTGGCTTTATGGGAC-3′	55.8	25	344
RhoA bw	5′-CCGTCTTTGGTCTTTGCTGAAC-3′			
RhoB fw	5′-GCATAAGGCAGCATTTTGACCAC-3′	52.9	25	323
RhoB bw	5′-GGAGGGGAATAAGGAAGAAGAAGC-3′			
Rac1 fw	5′-ACCGTCTTTGACAACTATTCTGCC-3′	56.5	25	366
Rac1 bw	5′-CTCCAGGTATTTGACAGCACCG-3′			
Cdc42 fw	5′-GTTGTTGTTGGTGATGGTGCTG-3′	54.4	25	372
Cdc42 bw	5′-GGCAAGTTTCTCAATAGTAGAGGGG-3′			
RhoGDI fw	5′-CGTTTGTGTTTGTCTGTGTGCG-3′	57.2	25	350
RhoGDI bw	5′-TCCACCCCATCACTTCCATTC-3′			

Table 2
Serum creatinine levels in ischemic and reperfused animals

	S30	I30	S90	R60
Creatinine (mg/L)	6.18 ± 0.23	8.22 ± 0.20‡	6.41 ± 0.25	16.48 ± 0.28‡
Animals (*n*)	6	12	6	12

Immediately after ischemia and reperfusion, blood was collected by intracardiac punction and serum was prepared. Serum creatinine levels were measured as indicated under Materials and methods and calculated as (mg/L) for each animal. The treatments undergone by the kidneys are S30 and S90: sham groups anesthetized and ventral operated for, respectively, 30 and 90 min, I30: ischemia for 30 min, R60: ischemia for 30 min followed by a reperfusion for 60 min. These results are expressed as means ± SEM. Significant differences (‡$p < 0.001$) compared their respective sham-operated rats.

[2,4,14]. To ensure the quality of isolated proximal tubules, their purity was confirmed by microscopic examination. In addition, enrichment of proximal tubule preparations was determined by measuring alkaline phosphatase activity, which was enriched 5-fold compared to cortex homogenates, without any difference between sham-operated and ischemic or reperfused kidneys (data not shown). As we reported, the transcriptional factor HIF-1α is induced by hypoxia in kidney cells [28]. We noted in the nuclear fractions from proximal tubules a 3-fold increase ($p < 0.05$) of HIF-1α level during ischemia (Fig. 1A). Thus, hypoxia is a key component in the unilateral reversible ischemic response and validates the model. Indeed, during reperfusion, HIF-1α returned to basal levels (Fig. 1A) since O_2 induced its proteolysis by the proteasome.

Actin cytoskeleton organization has been characterized by immunohistochemical techniques in renal epithelial cells upon ATP depletion [2]. Thus, the β-actin expression remained to be established during in vivo kidney ischemia. In whole proximal tubule homogenates, a reversible 30 min kidney ischemia significantly induced β-actin expression by 2.7-fold ($p < 0.01$) compared to sham-operated rats (Fig. 1B). The upregulation of β-actin expression was primarily located in nuclear fractions and increased 2.5-fold ($p < 0.01$). β-Actin levels were also examined in membrane fractions, Triton-soluble or not, since cytoskeletal proteins are expected to be enriched in Triton-insoluble fractions. In contrast to results seen with the nuclear fractions, there was a strong decrease in β-actin expression in crude membranes and in detergent-insoluble membranes by 47% ($p < 0.01$) and 42% ($p < 0.001$), respectively. During kidney reperfusion, β-actin levels in proximal tubule homogenates were about 2.2-fold ($p < 0.05$) those observed in sham-operated rats. This overexpressed β-actin during reperfusion was also present in nuclear fractions, which showed a 1.9-fold ($p < 0.05$) increase over the controls. Interestingly, reperfusion further inhibited β-actin levels in crude membranes by 74% ($p < 0.01$) and in Triton-insoluble membranes by 69% ($p < 0.001$). The decrease of β-actin in membranes was not accompanied by its accumulation in the soluble fractions during reperfusion. Together these data show that kidney ischemia stimulates β-actin expression in proximal tubules that accumulates in the nuclei and

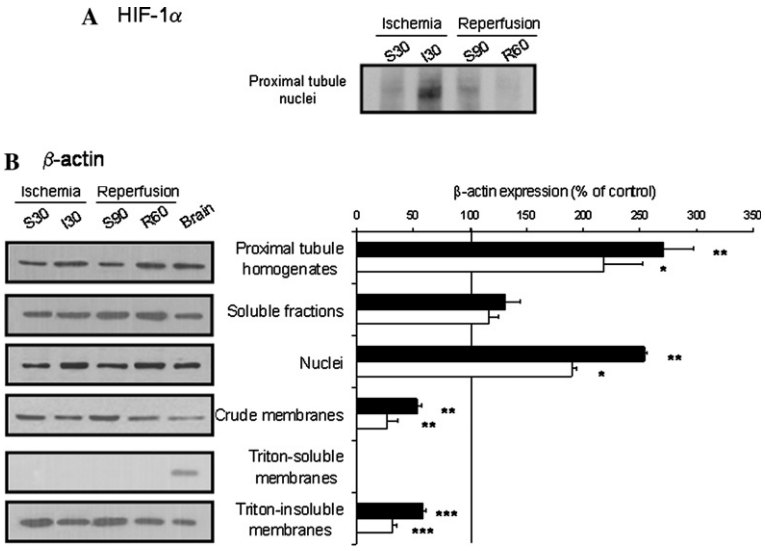

Fig. 1. Augmentation of HIF-1α and β-actin expression and redistribution of β-actin following kidney ischemia–reperfusion injury in proximal tubules. Proteins (25 μg) from proximal tubule fractions were separated by SDS–PAGE and analyzed by Western blotting to immunodetect HIF-1α (A) and β-actin (B) as described in Materials and methods. Representative blots of each proximal tubule fraction are shown. For each fraction, exposure times were different and signal produced on the blots was linear with respect to the protein loaded. The treatments undergone by the kidneys are identified at the top of the blots: S30 and S90: sham groups anesthetized and ventral operated for, respectively, 30 and 90 min, I30: ischemia for 30 min, and R60: ischemia for 30 min followed by a reperfusion for 60 min. β-Actin in brain was used as a positive control. The relative amounts of β-actin in proximal tubule fractions were determined by densitometric analysis. These data are expressed as percentages of respective sham controls and are means ± SEM of two experiments done in duplicate. (■) Ischemia and (□) reperfusion. *$p < 0.05$; **$p < 0.01$; and ***$p < 0.001$.

that membrane-bound β-actin is reduced under these conditions.

Specific effect of ischemia–reperfusion on tubulin subunit expression and distribution in proximal tubules

In whole homogenates, a very strong induction of α-tubulin expression occurred during kidney ischemia, where an increase of about 8.5-fold ($p < 0.001$) was observed (Fig. 2). This upregulation was also observed in nuclear fractions that experienced an increase of 8.8-fold ($p < 0.001$). There was also an increased expression, by 2-fold, in both crude membranes and Triton-insoluble membranes ($p < 0.001$). During kidney reperfusion, the α-tubulin level in proximal tubule homogenates was about 3.3-fold ($p < 0.001$) that in the sham-operated controls. On the other hand, there was a reduction in the amount of α-tubulin by about 25% ($p < 0.001$) in crude membranes, and in detergent-insoluble membranes ($p < 0.05$) compared to its sham-operated rats.

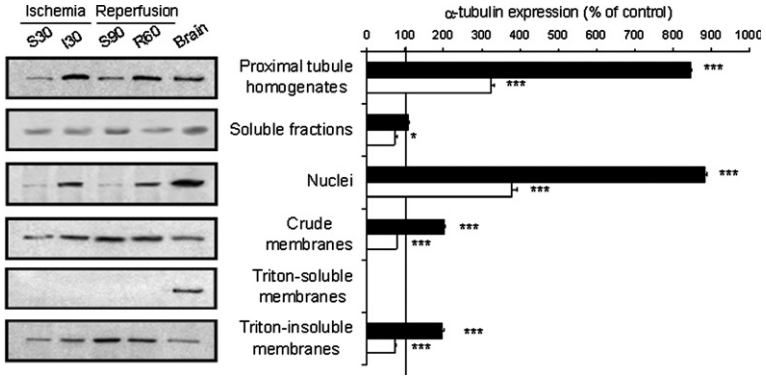

Fig. 2. Regulation of α-tubulin expression and distribution in proximal tubule fractions following kidney ischemia–reperfusion injury. Proteins (25 μg) from proximal tubule fractions were analyzed by Western blotting to immunodetect α-tubulin as described in Materials and methods. Representative blots of each proximal tubule fraction are shown. Exposure times were adjusted to each proximal tubule fraction and signal produced on the blots was linear with respect to the protein loaded. The treatments undergone by the kidneys are identified at the top of the blots as described in the legend to Fig. 1. α-Tubulin in brain served as positive control. The relative amounts of α-tubulin in proximal tubule fractions were measured by densitometric analysis. These data are expressed as percentages of respective sham controls and are means ± SEM of two experiments done in duplicate. (■) Ischemia and (□) reperfusion. *$p < 0.05$; and ***$p < 0.001$.

Ischemia and reperfusion exhibited different effects on β-tubulin expression and distribution. In proximal tubule homogenates, there was a slight increase in β-tubulin expression of 1.5-fold ($p < 0.001$) during ischemia compared to sham-operated rats (Fig. 3). Contrary to results obtained with α-tubulin, where the upregulated protein was observed in the nuclear fractions, the induced β-tubulin was found in soluble fractions where it increased by 1.4-fold ($p < 0.001$). As seen for α-tubulin, ischemia caused an inhibition of β-tubulin expression in crude and in Triton-insoluble membranes, where it diminished by 38 and 40% ($p < 0.01$), respectively, compared with controls. There are no significant differences in β-tubulin expression within the nuclear fractions during ischemia and reperfusion compared to their sham-operated controls. During reperfusion, β-tubulin levels were decreased by 24% ($p < 0.001$) in proximal tubule homogenates. Decreased expression was also seen in crude and in Triton-insoluble membranes, where β-tubulin levels diminished by about 25% ($p < 0.01$ and $p < 0.001$, respectively) during reperfusion. On the other hand, a small reperfusion-induced increase of 1.2-fold ($p < 0.05$) was observed in the soluble fractions of proximal tubules.

γ-Tubulin is the main component of the microtubule organizing center, the starting point of microtubule polymerization. The expression and distribution of γ-tubulin were not affected by ischemia or reperfusion in all proximal tubule fractions examined (Fig. 4). The lack of effect on γ-tubulin further demonstrates that ischemia and reperfusion specifically modulate each tubulin form in proximal tubules as well as β-actin expression.

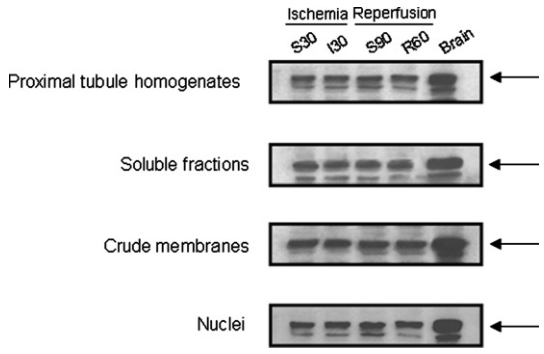

Fig. 4. Lack of effect of kidney ischemia–reperfusion injury on expression and distribution of γ-tubulin in proximal tubule fractions. Proteins (25 μg) from proximal tubule fractions were analyzed by Western blotting to immunodetect γ-tubulin as described in Materials and methods. Representative blots of each proximal tubule fraction are presented. Appropriate exposure times were different for each fraction and signal produced on the blots was linear with respect to the protein loaded. Kidney treatments are identified at the top of the blots as described in the Fig. 1 legend. γ-Tubulin in brain served as a positive control and it is identified by an arrow. These results are representative of two experiments done in duplicate.

Analysis of mRNA expression of β-actin, α-tubulin, and β-tubulin by RT-PCR in proximal tubules during ischemia–reperfusion injury

To gain insight into the molecular mechanisms upregulating cytoskeletal proteins in proximal tubules during renal ischemia, we next examined the effect of ischemia on mRNA levels. RNA was extracted from proximal tubules and analyzed by RT-PCR (data not shown). There was no difference in β-actin mRNA expression during ischemia and reperfusion between treated rats and their

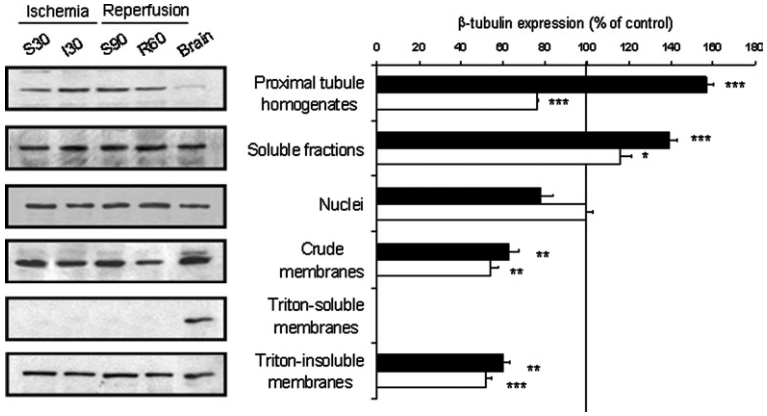

Fig. 3. Expression and distribution of β-tubulin in proximal tubule fractions during kidney ischemia–reperfusion injury. Proteins (25 μg) from proximal tubule fractions were analyzed by Western blotting. β-Tubulin was immunodetected as described in Materials and methods. Representative blots of each proximal tubule fraction are shown but exposure times varied and signal produced on the blots is linear with respect to the protein loaded. The treatments undergone by the kidneys are shown at the top of the blots and identified as described in the legend to Fig. 1. β-Tubulin in brain was employed as a positive control. The relative amounts of β-tubulin in proximal tubule fractions were determined by densitometry. These data are expressed as percentages of respective sham controls and are means ± SEM of two experiments done in duplicate. (■) Ischemia and (□) reperfusion. *$p < 0.05$; **$p < 0.01$; and ***$p < 0.001$.

sham-operated controls. Similarly, β-tubulin mRNA expression was stable during ischemia and reperfusion compared to sham-operated controls. In contrast, there was a strong increase in mRNA levels for α-tubulin in ischemia and, to a lesser degree, in reperfused proximal tubules. These data indicate that kidney ischemia upregulated β-actin and β-tubulin at the protein levels only, while α-tubulin expression was stimulated at both the mRNA and protein levels.

Upregulation of HSP70 in proximal tubules during ischemia–reperfusion

HSP73 has been recently shown to colocalize with microtubules and with perinuclear tubulin following cardiac ischemia [16]. During renal ischemia, HSP70 family protein expression was decreased in proximal tubule homogenates by 35% ($p < 0.05$) (Fig. 5). In contrast, its expression was strongly upregulated by 4.1-fold in the nuclear fractions ($p < 0.001$) and by 1.2-fold ($p < 0.01$) in crude membranes. During reperfusion, HSP70 expression was increased significantly in soluble fractions and in crude membranes by 1.6-fold ($p < 0.05$) and by 1.7-fold ($p < 0.01$).

Increased expression and redistribution of Rho GTPases in proximal tubules during ischemia–reperfusion

Since the Rho family of GTPases regulates actin cytoskeleton organization, their expression and distribution were analyzed in proximal tubules following kidney ischemia and reperfusion. In homogenates, RhoA expression was increased 2.8-fold ($p < 0.001$) by ischemia (Fig. 6A). In Triton-soluble membranes, RhoA levels were increased by 1.5-fold ($p < 0.05$) while ischemia reduced the amount of RhoA bound to detergent-insoluble membranes by 48% ($p < 0.001$). During reperfusion, RhoA levels decreased in homogenates by 31% ($p < 0.05$), in membrane fractions with an inhibition by 60% in crude membranes ($p < 0.01$), by 63% in Triton-soluble membranes ($p < 0.001$), and near-disappearance in Triton-insoluble membranes with an expression of only 6% ($p < 0.001$) compared to sham-operated controls.

We recently showed that RhoGDI is a key regulator for the inhibition of Rho GTPase activity, by extracting the phosphorylated Rho from biological membranes [27]. Ischemia caused a 4-fold increase ($p < 0.05$) in RhoGDI expression in homogenates. RhoGDI expression returned to control values during 60 min reperfusion in proximal tubule homogenates (Fig. 6B).

RhoB expression in proximal tubule homogenates tended to rise during ischemia (Fig. 7). This was observed in crude and in Triton-soluble membranes with a significant increase in RhoB expression by 1.8-fold ($p < 0.05$) and 1.7-fold ($p < 0.01$), respectively, compared to controls. Indeed, RhoB was completely absent in soluble fractions. During reperfusion, there is a decreased expression of 30% in the nuclear fraction ($p < 0.05$), of 49% in crude membranes ($p < 0.01$), and of 36% in membranes which are soluble in detergent ($p < 0.01$). RhoB was not present in Triton-insoluble membranes, suggesting that this GTPase is not associated with the cytoskeleton.

Cdc42 expression and distribution were studied in proximal tubules and are shown in Fig. 8. Ischemia triggered an increase in Cdc42 expression in crude membranes by 1.9-fold ($p < 0.001$). This upregulation was primarily found in Triton-soluble membranes which exhibited an increase of 1.6-fold ($p < 0.001$). In contrast, Cdc42 expression was diminished in Triton-insoluble membranes by 41% compared to sham-operated controls ($p < 0.01$). Reperfusion reduced the level of this

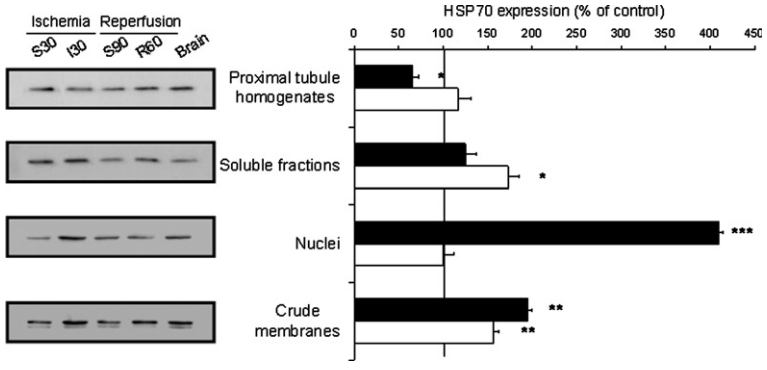

Fig. 5. Alteration of HSP70 expression and distribution in proximal tubule fractions following kidney ischemia–reperfusion injury. Proteins (25 μg) from proximal tubule fractions were analyzed by Western blotting. HSP70 was immunodetected as described in Materials and methods. Representative blots of each proximal tubule fraction are shown but exposure times varied and signal produced on the blots was linear with respect to the protein loaded. The treatments undergone by the kidneys are shown at the top of the blots and identified as described in the legend to Fig. 1. HSP70 in brain was employed as a positive control. The relative amounts of HSP70 in proximal tubule fractions were determined by densitometry. These data are expressed as percentages of respective sham controls and are means ± SEM of two experiments done in duplicate. (■) Ischemia and (□) reperfusion. *$p < 0.05$; **$p < 0.01$; and ***$p < 0.001$.

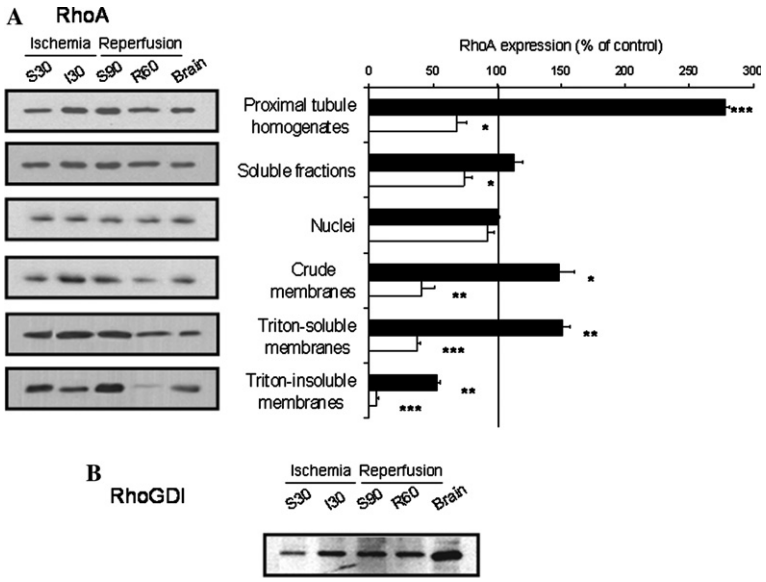

Fig. 6. Upregulation of RhoA and RhoGDI expression and distribution following kidney ischemia–reperfusion injury in proximal tubule fractions. Proteins (25 μg) from proximal tubule fractions were analyzed by Western blotting to immunodetect RhoA (A) and RhoGDI (B) as described in Materials and methods. Representative blots of each proximal tubule fraction are shown with appropriate exposure times for each and signal produced on the blots was linear with respect to the protein loaded. Treatments of kidneys are identified at the top of the blots as described in the legend to Fig. 1. RhoA and RhoGDI in brain were used as a positive control. The relative amounts of RhoA in proximal tubule fractions were quantified by densitometric analysis. These data are expressed as percentages of respective sham controls and are means ± SEM of two experiments done in duplicate. (■) Ischemia and (□) reperfusion. *$p < 0.05$; **$p < 0.01$; and ***$p < 0.001$.

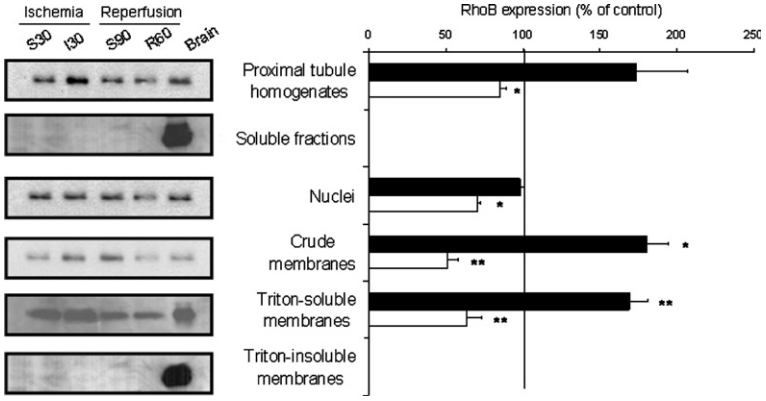

Fig. 7. Regulated expression of RhoB in proximal tubule fractions by kidney ischemia–reperfusion injury. Proteins (25 μg) from proximal tubule fractions were analyzed by Western blotting to immunodetect RhoB as described in Materials and methods. Representative blots of each proximal tubule fraction are shown. For each fraction, appropriate exposure times were used and signal produced on the blots was linear with respect to the protein loaded. Kidney treatments are identified at the top of the blots as described in Fig. 1 legend. RhoB in brain was used as a positive control. The relative amounts of RhoB in proximal tubule fractions were evaluated by densitometric analysis. These data are expressed as percentages of respective sham controls and are means ± SEM of two experiments done in duplicate. (■) Ischemia and (□) reperfusion. *$p < 0.05$; and **$p < 0.01$.

GTPase by 46% in crude membranes ($p < 0.01$), by 58% in Triton-soluble membranes ($p < 0.001$), and led to its disappearance in Triton-insoluble membranes with an expression of only 5% ($p < 0.001$) compared to controls.

Finally, in proximal tubule homogenates, Rac1 expression was increased nearly 2-fold by a 30 min reversible ischemia ($p < 0.01$) (Fig. 9). Rac1 expression was also slightly increased in Triton-soluble membranes during ischemia, by 1.5-fold ($p < 0.01$). However, Rac1 expression decreased by 65% ($p < 0.001$) in Triton-insoluble membranes, compared to sham-operated rats, during ischemia. In contrast to other Rho GTPases, reperfusion triggered a marked expression of Rac1 in soluble fractions by more than 4-fold ($p < 0.05$). On the other hand, Rac1 expression was diminished by 42% in crude membranes ($p < 0.05$) and by 65% in detergent-soluble membranes ($p < 0.01$). Moreover, Rac1 almost disappeared in Triton-insoluble membranes since an expression of only 20% of the control levels ($p < 0.001$) was observed during reperfusion.

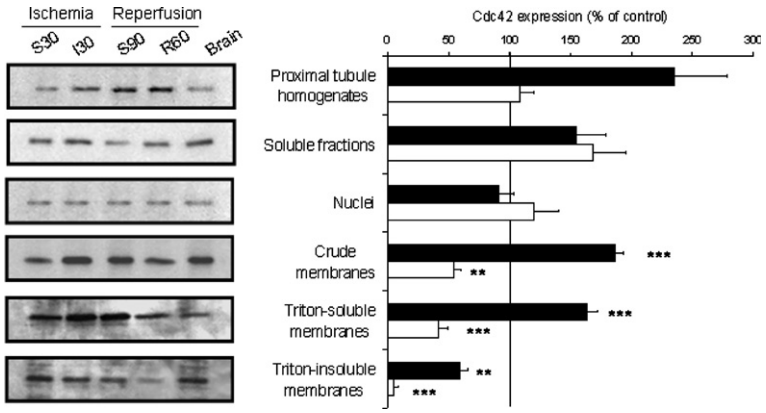

Fig. 8. Upregulation of expression and distribution of GTPase Cdc42 in proximal tubule fractions by kidney ischemia–reperfusion injury. Proteins (25 μg) from proximal tubule fractions were analyzed by Western blotting to immunodetect Cdc42 as described in Materials and methods. Representative blots of each proximal tubule fraction are presented. Exposure times were adjusted for each fraction and signal produced on the blots was linear with respect to the protein loaded. Treatments undergone by the kidneys are identified at the top of the blots as described in Fig. 1 legend. Cdc42 in brain was used as a positive control. The relative amounts of Cdc42 in proximal tubule fractions were assessed by densitometric analysis. These data are expressed as percentages of respective sham controls and are means ± SEM of two experiments done in duplicate. (■) Ischemia and (□) reperfusion. $^{**}p < 0.01$; and $^{***}p < 0.001$.

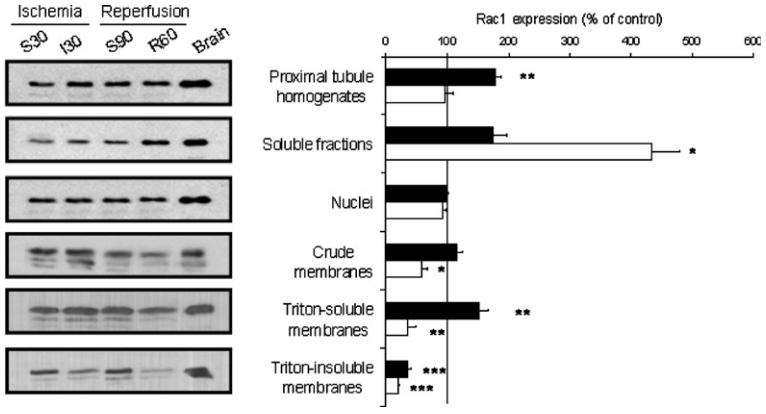

Fig. 9. GTPase Rac1 expression and distribution in proximal tubule fractions during kidney ischemia–reperfusion injury. Proteins (25 μg) from proximal tubule fractions were analyzed by Western blotting and then Rac1 was immunodetected as described in Materials and methods. Representative blots of each proximal tubule fraction are shown. For each fraction, an appropriate exposure time was used and signal produced on the blots was linear with respect to the protein loaded. Treatments to which kidneys were submitted are identified at the top of the blots as described in the legend to Fig. 1. Rac1 in brain was used as a positive control. The relative amounts of Rac1 in proximal tubule fractions were determined by densitometric analysis. These data are expressed as percentages of respective sham controls and are means ± SEM of two experiments done in duplicate. (■) Ischemia and (□) reperfusion. $^{*}p < 0.05$; $^{**}p < 0.01$; and $^{***}p < 0.001$.

mRNA expression of Rho GTPases is regulated by ischemia–reperfusion in proximal tubules

RT-PCR analysis of Rho GTPases mRNA expression is shown in Fig. 10. For each GTPases, RhoA, RhoB, Rac1, and Cdc42, ischemia increased mRNA expression compared to their sham-operated controls. In contrast, there were no differences in RhoA and Rac1 mRNA levels between reperfused and control proximal tubules. There was a slight diminution in the RhoB mRNA level during reperfusion. However, Cdc42 mRNA was higher in reperfused proximal tubules than in controls. Thus, changes at the mRNA levels of Rho GTPases agreed with those seen at the protein levels. For RhoGDI, mRNA level appeared slightly stimulated by ischemia. β-Actin mRNA levels were unaffected by ischemia and reperfusion compared to their controls, showing the specificity of Rho GTPases and RhoGDI mRNA regulation under these conditions.

ERM protein expression is not regulated by ischemia–reperfusion in proximal tubules

ERM proteins function as plasma membrane-actin cytoskeleton linkers and participate in the formation of specialized domains of the plasma membrane in proximal tubules known as microvilli. The antibody used for immunodetection recognized both ezrin and radixin

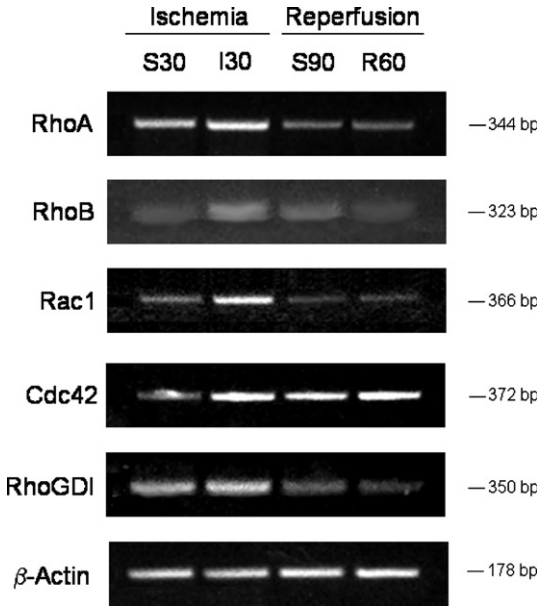

Fig. 10. RT-PCR analysis of mRNA expression for Rho GTPases and their regulator RhoGDI during ischemia–reperfusion injury. Total RNA extracted from proximal tubules (1 μg) was analyzed by RT-PCR to assess mRNA levels of RhoA, RhoB, Cdc42, Rac1, RhoGDI, and β-actin as described in Materials and methods and Table 1. Treated kidneys are: S30 and S90: sham groups, anesthetized and ventral operated for, respectively, 30 and 90 min, I30: ischemia for 30 min, and R60: ischemia for 30 min followed by a reperfusion for 60 min. These results are representative of three experiments.

co-migrating at a molecular weight of 80 kDa as well as moesin at 78 kDa. The expression and distribution of ezrin–radixin and moesin were not affected in the soluble fractions or crude membranes from proximal tubules following ischemia and reperfusion injury ($p > 0.05$) (Fig. 11A). Although total ezrin–radixin levels immunodetected at 80 kDa remained stable during ischemia–reperfusion, this did not exclude the possibility, but it is unlikely, that their individual expression could be regulated in an opposite manner that exactly compensated for the expression of each other protein. Thus, ERM proteins responded differently in a living animal compared to previous studies where they were released from membranes in isolated proximal tubules incubated upon anoxia and chemical ATP depletion [8,9].

Occludin is a protein component of tight junctions [29] and ischemia has been reported to alter functional integrity of tight junctions [30–32]. RhoA can regulate occludin phosphorylation and tight junction permeability [33]. Occludin expression decreased in proximal tubule homogenates and in crude membranes by 32% ($p < 0.05$) and by 29% ($p < 0.01$), respectively, during ischemia (Fig. 11B). During reperfusion, occludin expression was strongly decreased by 63% ($p < 0.01$) in crude membranes while the level of this tight junction protein was not affected during reperfusion in proximal tubule homogenates. Occludin was not detected in the soluble fractions.

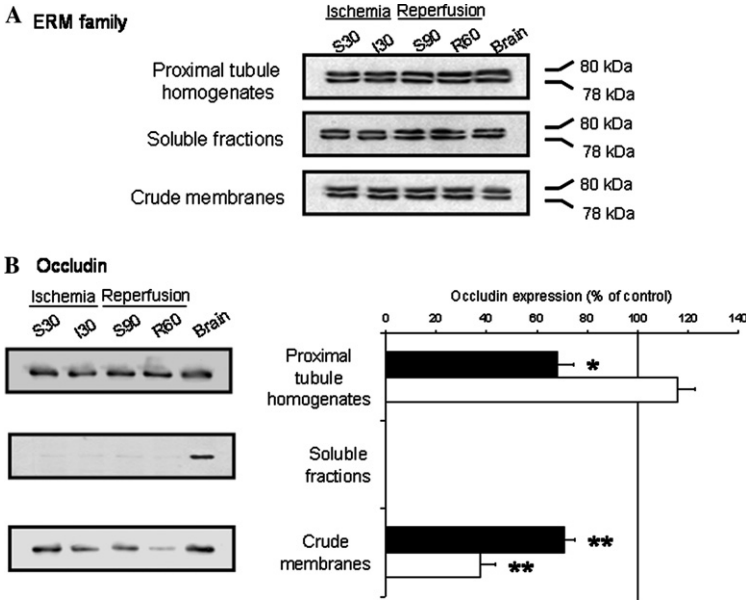

Fig. 11. Impact of kidney ischemia–reperfusion injury on expression and distribution of ERM proteins and occludin in proximal tubule fractions. Proximal tubule fractions (proteins 25 μg) were analyzed by Western blotting to immunodetect ezrin–radixin and moesin (A) and occludin (B) as described in Materials and methods. Representative blots of each proximal tubule fraction are shown with appropriate exposure times for each and signal produced on the blots was linear with respect to the protein loaded. Treatments of kidneys are identified at the top of the blots as described in the legend to Fig. 1. Ezrin–radixin–moesin and occludin in brain were used as a positive control. The relative amounts of occludin in proximal tubule fractions were quantified by densitometric analysis. These data are expressed as percentages of respective sham controls and are means ± SEM of two experiments done in duplicate. (■) Ischemia and (□) reperfusion. *$p < 0.05$; **$p < 0.01$.

Upregulation of caveolin-1 expression and its distribution in proximal tubules during kidney ischemia–reperfusion

We have shown that some GTPases are located in caveolae, which are membrane microdomains enriched in signaling molecules [32]. Consequently, caveolin-1 expression and distribution were assessed during kidney ischemia and reperfusion. Ischemia induced caveolin-1 expression by 2.8-fold ($p < 0.001$) in proximal tubule homogenates (Figs. 12A and B). More specifically, caveolin-1 upregulation occurred in membranes. Caveolin-1 expression was increased in crude membranes by 3.1-fold ($p < 0.001$) and in Triton-soluble membranes by 3.2-fold ($p < 0.001$) compared to sham-operated rats. However, caveolin-1 expression was reduced in Triton-insoluble membranes by 55% during reversible ischemia ($p < 0.001$). During reperfusion, the caveolin-1 level was 1.6-fold ($p < 0.01$) greater than in controls. In crude membranes and in Triton-soluble membranes, caveolin-1 expression was upregulated by 1.6-fold ($p < 0.01$). In Triton-insoluble membranes, caveolin-1 almost disappeared with an expression of only 16 % ($p < 0.001$) of that found in sham-operated controls. Expression of both α- and β-caveolin-1 isoforms was similarly modulated by ischemia and reperfusion (Fig. 12A).

Although Triton-insolubility of caveolae is criterion for their purification [45], our results in proximal tubules indicated that membrane-bound caveolin-1 was predominantly in the Triton-soluble fractions and that the upregulated caveolin-1 during ischemia was also associated with Triton-soluble membranes. To support our observations on caveolin-1 cellular distribution, we examined various conditions for preparing the Triton-soluble and Triton-insoluble membranes from proximal tubules as shown in Fig. 12B. The partition of caveolin-1 and β-actin, used as a control, between the two membrane fractions was not affected by the incubation temperature (4 or 37 °C) and by the ionic strength (0 or 150 mM KCl) where 4 °C and 150 mM are representing caveolae usual preparation conditions [45]. These data demonstrate that the presence of caveolin-1 in Triton-soluble membranes was independent of the method used for preparing the membranes, but was a property of caveolin-1 in proximal tubule membranes. In some cell lines, caveolin-1 is associated with the Golgi membranes in addition to caveolae [46]. We therefore determined

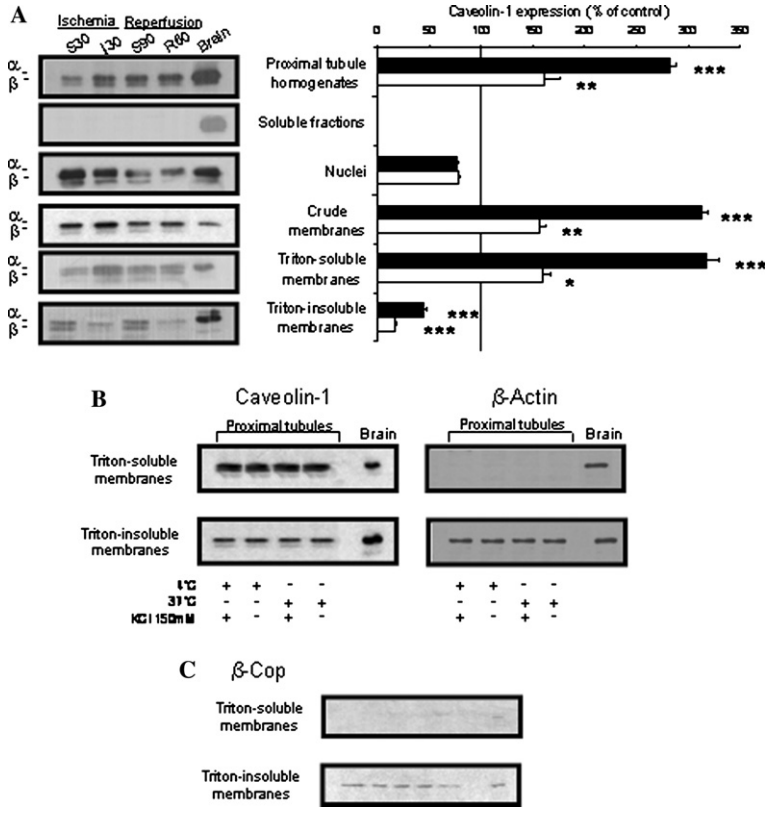

Fig. 12. Increased expression and distribution of caveolin-1 in proximal tubule fractions following kidney ischemia–reperfusion injury. Proximal tubule fraction proteins (25 μg) were analyzed by Western blotting to immunodetect caveolin-1 as described in Materials and methods. For each fraction, an appropriate exposure time was used and signal produced on the blots was linear with respect to the protein loaded. (A) The relative amounts of caveolin-1, α- and β-subunits together in proximal tubule fractions were determined by densitometric analysis. These data are expressed as percentages of respective sham controls and are means ± SEM of two experiments done in duplicate. (■) Ischemia and (□) reperfusion. *$p < 0.05$; **$p < 0.01$ and ***$p < 0.001$. (B) Effects of salt and temperature on solubilization of caveolin-1 from crude membranes incubated in Triton X-100. (C) Localization of β-Cop, a Golgi marker, in solubilized crude membranes in the presence of Triton X-100.

whether Golgi proteins were localized in Triton-soluble or Triton-insoluble membranes by monitoring the immunodetection of β-COP, a Golgi marker (Fig. 12C). β-COP was only observed in Triton-insoluble membranes, indicating that most of the caveolin-1 in proximal tubules was not associated to Golgi but to Triton-soluble membranes.

Discussion

The animal model used in this study employs acute renal ischemia for 30 min followed, or not, by a brief 60 min period of reperfusion. Thirty minutes ischemia was selected because it is below the 45 min limit previously reported as the longest period of renal warm ischemia allowing reversible injury and compatible with survival [47]. Purity of isolated proximal tubules was confirmed by microscopic examination. We showed that combined ischemia–reperfusion treatment led to renal failure since the serum creatinine level increases under these conditions (Table 2). Moreover, this well-characterized and documented model has been used in several studies measuring the impact of ischemic–reperfusion injury at the histological, physiological, biochemical, and molecular levels [2,4,14]. In some proximal tubule fractions, levels of immunodetected proteins or mRNA differ between animals that have been sham-operated for 30 min (S30) and for 90 min (S90). This is likely explained by the different quantities of anesthetic administered to the rats. Since ischemic and sham S30 rats were anesthetized for only 30 min, they required less anesthetic than did the reperfused and sham S90 animals that were anesthetized for a total of 90 min. There were no differences in anesthetic quantity between ischemic and S30 rats or between reperfused and S90 rats, allowing direct comparison between treated and control rats.

The increased levels of HIF-1α were known to be induced by hypoxia in cultured renal cells [28] and we observed it in the nuclear fractions of proximal tubules by ischemia (Fig. 1A), indicating a hypoxic component in the ischemic response. Its presence at low levels in sham-operated animals could arise from either the xylazine anesthesia or the carbon dioxide lethal exposure. Adverse effects of xylazine include acidosis, hypercardia, hypotension, and hypoxia, even at a dosage as low as 7 mg/kg [48]. Moreover, CO_2 exposure has been demonstrated to induce HIF-1α levels in rat kidneys [49]. During reperfusion, HIF-1α disappearance could be explained by its proteasomal degradation following the massive oxygen arrival in kidney. The HIF-1α reperfusion-induced degradation has also been observed in other tissues such as the lung [50] and the liver [51].

Previous studies used immunohistological techniques to analyze ischemic effects on actin polymerization and organization [5,6]. Our findings, showing an upregulation of β-actin levels, are the first observations demonstrating that not only β-actin distribution but also its expression is regulated by ischemia. Ischemia-induced β-actin accumulates in nuclear fractions. Interestingly, this observation is supported by data showing that proximal tubule injury leads to actin depolymerization where actin microfilaments collapse on the nuclei. For instance, an induced chemical ATP depletion for 30 min causes a thinning of F-actin in microvilli, cortical region, and basal stress fibers, with the concurrent appearance of F-actin patches near the nucleus [52]. This actin collapse could be a physiological mechanism of nuclear protection. Among other mechanisms, actin microfilament depolymerization and collapse is likely mediated by actin depolymerizing factor (ADF). ADF, also known as cofilin, binds to actin in order to depolymerize it and it has been reported that ischemia caused ADF activation through dephosphorylation [2]. Moreover, ADF activation and relocalization toward apical actin was characterized as an early event occurring before actin alterations [53]. Thus, ADF appears as a key player for actin depolymerization during renal ischemia.

An additional cytoskeletal component important for cellular polarity and protein trafficking is microtubules. A previous study demonstrated that a light depolymerization of microtubules in epithelial cells occurs after 40 min kidney ischemia and that this alteration is still detectable after 1 h of reperfusion [14]. A similar observation has been made in liver after ischemia–reperfusion injury [54]. In this study, we investigated the effects of kidney ischemia on the expression of α-, β-, and γ-tubulin at the protein and mRNA levels as well as their subcellular location in proximal tubules following the injury. Tubulin polymerization is an intricate phenomenon under complex regulation where an initiation step precedes the nucleation step. Microtubule formation occurs by continuous assembly and disassembly of α- and β-tubulin heterodimers. Our results suggest that the induced α- and β-tubulin do not participate in microtubule polymerization during ischemia because there is much more induction of α-tubulin than β-tubulin, with increases of 8.5-fold and 1.6-fold, respectively (Figs. 2 and 3). In addition, their localizations are different with α-tubulin accumulating in nuclear fractions while β-tubulin remains in soluble fractions. Supporting this assumption, GTP levels are depleted by 90% after 30 min kidney ischemia in rats [55], likely impairing microtubule polymerization.

A possible mechanism explaining the presence of α-tubulin in the nuclear fractions could be the formation of α-tubulin-HSP complexes. For example, tubulin and microtubules are associated with HSP27 in HeLa cells [56]. It has also been noted that HSP90 binds in vitro to tubulin dimers [57], and that tubulin complexes with HSP73 in canine myocardium [16]. These complexes are mainly observed in the perinuclear region [26,56,57].

Moreover, several HSP are known to collapse toward nuclei during ischemic insults in different tissues [58]. In our current study, we observed an increase of HSP70 in nuclear fraction from ischemic proximal tubules which is consistent with our hypothesis.

γ-Tubulin is the main component of the microtubule organizing center, the starting point of microtubule nucleation in vivo [59]. While α-tubulin is upregulated at both the mRNA and protein levels and β-tubulin is slightly stimulated at the protein level only, γ-tubulin expression and distribution are unaffected by ischemia–reperfusion injury. Thus, microtubule organizing centers containing γ-tubulin should retain their microtubule nucleation capacity upon ischemia and reperfusion. Finally, the absence of regulation by ischemia and reperfusion on this housekeeping protein is showing the specificity of β-actin, α-tubulin, β-tubulin, and Rho GTPases regulation under these conditions.

Ischemia increases the expression of RhoA, RhoB, Cdc42, and Rac1 at the mRNA and protein levels, but these induced Rho GTPases are mainly associated with Triton-soluble membranes. In addition, this is accompanied by a reduction of Rho GTPases found in Triton-insoluble membranes suggesting that they are released from caveolae or cytoskeleton during ischemia. Data supporting that Rho GTPases may be inactivated is actin depolymerization observed during ischemia [5,6]. Published reports also support this assumption that RhoA, Rac1, and Cdc42 are inactivated by ischemia. First, chemical ATP depletion was reported to cause Rho GTPases inactivation [24]. Moreover, during ischemia, GTP depletion could inactivate Rho GTPases functions [25]. Furthermore, during chemical ATP depletion of cells transfected with a constitutively active form of RhoA there is a protection against actin depolymerization; supporting the hypothesis that ischemia induces Rho GTPases inactivation [60]. Finally, when associated with caveolae which are Triton-insoluble membranes, Ras or Rho GTPases are shown to be inactive. Upon cell stimulation, Rho and Ras proteins are released from caveolae and they are activated [61–63]. However, caveolar disruption has been demonstrated to prevent such activation [64] and caveolae have been reported to be disrupted upon ischemia [39], supporting that Rho GTPases could be inactivated under these conditions. Thus, the upregulation of Rho GTPases in proximal tubules during kidney ischemia is possibly a compensating response to overcome their inhibition resulting from cellular stresses.

Besides the effect on the regulation of cytoskeleton organization, inhibition of Rho proteins during ischemia–reperfusion should disrupt several cell processes since these small GTPases control and integrate several downstream pathways involved in cell cycle progression, apoptosis and modulate the transcription of specific genes. However, the consequences of Rho inactivation on these processes remain to be characterized during renal ischemia–reperfusion injury. Interestingly, our laboratory recently demonstrated that 1–4 h of hypoxia (1% O_2) treatments lead to the increased expression of Cdc42, Rac1, and RhoA by 2–4-fold in cultured renal cell carcinoma. In addition, we showed that this increase of Rho GTPases is a necessary regulator of the cascade leading to HIF-1α accumulation [28]. Thus, hypoxia could be a critical factor for the stimulation of Rho GTPases expression in renal ischemic response.

Previously, we reported that RhoA is associated with caveolae and binds to caveolin-1 [34]. During kidney ischemia, there is a 2.8-fold increase in caveolin-1 expression. In addition, there is a reduction of caveolin-1 in Triton-insoluble membranes accompanied by an increase in Triton-soluble membranes as observed here for Rho GTPases. Similar results have been observed during acute renal failure [39]. Caveolin-1 has been described as cycling between the plasma membranes and the Golgi by a multi-step process requiring microtubules in one of the steps [46]. The accumulation of caveolin-1 in Triton-soluble membranes could result from microtubule network depolymerization, impairing its transport. Furthermore, caveolin-1 release from Triton-insoluble membranes also suggests caveolar disruption during ischemia. This possible disruption of caveolae during ischemia supports our hypothesis of inactivation of Rho GTPases under these conditions.

Ischemia induced a profound accumulation of RhoA, RhoB, and Cdc42 in crude membranes of proximal tubules. Upon reperfusion, these amounts were strongly reduced, not to basal levels, but to levels half those of sham-operated rats. For instance, the decrease for membrane-bound RhoA is not accompanied by a concomitant increase in the soluble fraction since this GTPase also decreases in this fraction. These observations suggest that during reperfusion there is a rapid proteolysis of ischemia-induced and also some constitutively expressed Rho GTPases. Since most of Rho GTPases are likely under an inactive state, their proteolysis should be an attempt to regulate their level and activity, allowing a fine-tuning of the cytoskeleton organization under these new physiological conditions associated to reperfusion.

RhoB differs from the other Rho family GTPases since it is exclusively found in membranes [65]. In our study, RhoB mRNA and protein are induced slightly but not significantly. In agreement with our observations in proximal tubules, RhoB was shown elsewhere to be rapidly upregulated, as measured by cDNA expression array, in ischemic mouse brain and this upregulation was also observed at the protein level [66]. Interestingly, our study demonstrates, for the first time, that RhoB is found in Triton-soluble membranes in controls and in ischemic proximal tubules, suggesting that these membranes contain both active and inactive forms of RhoB.

During reperfusion, Rac1 expression strongly increases in the soluble fractions (4.5-fold) but its mRNA level is induced during ischemia only. In contrast to other Rho proteins, Rac1 is the only Rho GTPase that seems to undergo a translocation from membranes to the soluble fraction during reperfusion. Several lines of evidence suggest that a burst of reactive oxygen species (ROS) generation coincides with reperfusion [67]. This production of ROS appears to require the participation of Rac1 [68]. Inhibition of Rac1 by the use of a dominant negative form of Rac1 protects against ROS [69]. Thus, the upregulation of Rac1 levels in the soluble fraction during reperfusion could be related to ROS generation in reperfused proximal tubules.

ERM proteins bind to actin and are regulated by Rho GTPases. Hypoxia or chemical ATP depletion resulted in ERM family protein redistribution from membranes to the soluble fraction in isolated proximal tubules [7]. This phenomenon is not observed in proximal tubules purified from rat ischemic kidneys. The ERM phosphorylation state regulates their localization since they are found in the soluble fractions when dephosphorylated [70]. The threonine phosphatase responsible for ERM dephosphorylation has been identified as protein phosphatase 2A (PP2A) [71]. It has been demonstrated that PP2A activity decreases during ischemia and reperfusion [72]. Therefore, these data suggest that ERM proteins may not be dephosphorylated since PP2A should be inhibited during ischemia and reperfusion in this in vivo model.

Component of tight junctions, occludin, was reduced in crude membranes upon ischemia and reperfusion. This reduction may be explained by MMP-9 activity which is known to be increased during ischemia [32,73,74]. This conclusion is supported by the observation that the extracellular domain of tight junction proteins was degraded during cerebral ischemia, but that this was reduced in MMP-9 knock-out mice [32]. Moreover, occludin has been recently associated with the MMP-9 induced perturbation of tight junction barrier in rats' testis [75]. Furthermore, ischemia, by other mechanisms, impaired tight junction integrity whether by an upregulation in calcium efflux [76] or by tight junction proteins becoming less soluble [77].

In conclusion, reversible renal ischemia and reperfusion noticeably induced actin and microtubule cytoskeleton components in addition to Rho GTPases regulating actin cytoskeleton, suggesting that they participate in an adaptive response to cellular lesions.

Acknowledgments

Financial support was provided by grants from the Canadian Institution of Health Research and Groupe de therapie experimentale du cancer de montreal (to R.B.) and from the Natural Sciences and Engineering Research Council of Canada (to R.R.D.). We thank Dr Borhane Annabi for his critical reading of the manuscript.

References

[1] F. Liano, J. Pascual, Kidney Int. 50 (1996) 811–818.
[2] N. Schwartz, M. Hosford, R.M. Sandoval, M.C. Wagner, S.J. Atkinson, J. Bamburg, B.A. Molitoris, Am. J. Physiol. 276 (1999) F544–F551.
[3] T.A. Sutton, B.A. Molitoris, Semin. Nephrol. 18 (1998) 490–497.
[4] B.A. Molitoris, J. Leiser, M.C. Wagner, Pediatr. Nephrol. 11 (1997) 761–767.
[5] P.S. Kellerman, R.T. Bogusky, Kidney Int. 42 (1992) 896–902.
[6] D. Brown, R. Lee, J.V. Bonventre, Am. J. Physiol. 273 (1997) F1003–F1012.
[7] J. Chen, R.B. Doctor, L.J. Mandel, Am. J. Physiol. 267 (1994) C784–C795.
[8] J. Chen, J.A. Cohn, L.J. Mandel, Proc. Natl. Acad. Sci. USA 92 (1995) 7495–7499.
[9] J. Chen, M.C. Wagner, Am. J. Physiol. 280 (2001) F619–F627.
[10] R. Bacallao, Semin. Nephrol. 15 (1995) 285–290.
[11] R.H. Wade, A.A. Hyman, Curr. Opin. Cell Biol. 9 (1997) 12–17.
[12] A. Desai, T.J. Mitchison, Annu. Rev. Cell Dev. Biol. 13 (1997) 83–117.
[13] M. Caplow, J. Shanks, J. Biol. Chem. 265 (1990) 8935–8941.
[14] M. Abbate, J.V. Bonventre, D. Brown, Am. J. Physiol. 267 (1994) F971–F978.
[15] W.E. Smoyer, R. Ransom, R.C. Harris, M.J. Welsh, G. Lutsch, R. Benndorf, J. Am. Soc. Nephrol. 11 (2000) 211–221.
[16] R.S. Decker, M.L. Decker, S. Nakamura, Y.S. Zhao, S. Hedjbeli, K.R. Harris, F.J. Klocke, Am. J. Physiol. Heart Circ. Physiol. 283 (2002) H1322–H1333.
[17] A. Hall, Science 279 (1998) 509–514.
[18] D. Boivin, D. Bilodeau, R. Beliveau, Can. J. Physiol. Pharmacol. 74 (1996) 801–810.
[19] C.D. Nodes, A. Hall, Biochem. Soc. Trans. 23 (1995) 456–459.
[20] A.J. Ridley, A. Hall, Cell 70 (1992) 389–399.
[21] A.J. Ridley, H.F. Paterson, C.L. Johnson, D. Diekmann, A. Hall, Cell 70 (1992) 401–410.
[22] M. Amano, Y. Fukata, K. Kaibuchi, Trends Cardiovasc. Med. 8 (1998) 162–168.
[23] A. Best, S. Ahmed, R. Kozma, L. Lim, J. Biol. Chem. 271 (1996) 3756–3762.
[24] N. Raman, S.J. Atkinson, Am. J. Physiol. 276 (1999) C1312–C1324.
[25] M.A. Hallett, P.C. Dagher, A.J. Atkinson, Am. J. Physiol. Cell Physiol. 285 (2003) C129–C138.
[26] A. Togawa, J. Miyoshi, H. Ishizaki, M. Tanaka, A. Takakura, H. Nishioka, H. Yoshida, T. Doi, A. Mizoguchi, N. Matsuura, Y. Niho, Y. Nishimune, Si. Nishikawa, Y. Takai, Oncogene 18 (1999) 5373–5380.
[27] M.A. Forget, R.R. Desrosiers, D. Gingras, R. Béliveau, Biochem. J. 361 (2002) 243–254.
[28] S. Turcotte, R.R. Desrosiers, R. Béliveau, J. Cell Sci. 116 (2003) 2247–2260.
[29] M. Furuse, T. Hirase, M. Itoh, A. Nagafuchi, S. Yonemura, S. Tsukita, S. Tsukita, J. Cell Biol. 123 (1993) 1777–1788.
[30] P.E. Canfield, A.M. Geerdes, B.A. Molitoris, Am. J. Physiol. 261 (1991) F1038–F1045.
[31] V.M. Kroshian, A.M. Sheridan, W. Lieberthal, Am. J. Physiol. 266 (1994) F21–F30.
[32] M. Asahi, X. Wang, T. Mori, T. Sumii, J.-C. Jung, M.A. Moskowitz, M.E. Fini, E.H. Lo, J. Neurosci. 21 (2001) 7724–7732.

[33] T. Hirase, S. Kawashima, E.Y. Wong, T. Ueyama, Y. Rikitake, S. Tsukita, M. Yokoyama, J.M. Staddon, J. Biol. Chem. 276 (2001) 10423–10431.
[34] D. Gingras, F. Gauthier, S. Lamy, R.R. Desrosiers, R. Béliveau, Biochem. Biophys. Res. Commun. 247 (1998) 888–893.
[35] C.J. Fielding, P.E. Fildering, Biochim. Biophys. Acta 1529 (2000) 210–222.
[36] T. Okamoto, A. Schlegel, P.E. Scherer, M.P. Lisanti, J. Biol. Chem. 273 (1998) 5419–5422.
[37] M. Stahlhut, B. van Deurs, Mol. Biol. Cell 11 (2000) 325–337.
[38] D.I. Mundy, T. Machleidt, Y.S. Ying, R.G. Anderson, G.S. Bloom, J. Cell Sci. 115 (2002) 4327–4339.
[39] R.A. Zager, A. Johnson, S. Hanson, V. Dela Rosa, Kidney Int. 61 (2002) 1674–1683.
[40] M. Essig, M. Vrtovsnik, G. Nguyen, J.D. Sraer, G. Friedlander, J. Am. Soc. Nephrol. 9 (1998) 1377–1388.
[41] R.R. Desrosiers, F. Gauthier, J. Lanthier, R. Beliveau, J . Biol. Chem. 275 (2000) 14949–14957.
[42] P.K. Smith, R.I. Krohn, G.T. Hermanson, A.K. Mallia, F.H. Gartner, M.D. Provenzano, E.K. Fujimoto, N.M. Goeke, B.J. Olson, D.C. Klenk, Anal. Biochem. 150 (1985) 76–85.
[43] U.K. Laemmli, Nature 227 (1970) 680–685.
[44] R.R. Desrosiers, F. Gauthier, J. Lanthier, R. Béliveau, J. Biol. Chem. 275 (2000) 14949–14957.
[45] D.A. Brown, J.K. Rose, Cell 68 (1992) 533–544.
[46] P.A. Conrad, E.J. Smart, Y.S. Ying, R.G. Anderson, G.S. Bloom, J. Cell Biol. 131 (1995) 1421–1433.
[47] S.C. Weight, P.N. Furness, M.L. Nicholson, Br. J. Surg. 85 (1998) 1669–1673.
[48] S.K. Wixson, W.J. White, H.S. Hughes, Lab. Anim. Sci. 37 (1987) 736–742.
[49] C. Rosenberg, S. Mandriota, J.S. Jurgensen, M.S. Wiesener, J.H. Horstrup, U. Frei, P.J. Ratcliffe, P.H. Maxwell, S. Bachmann, K.U. Eckardt, J. Am. Soc. Nephrol. 13 (2002) 1721–1732.
[50] A.Y. Yu, M.G. Frid, L.A. Shimoda, C.M. Wiener, K. Stenmark, G.L. Semenza, Am. J. Physiol. Lung Cell. Mol. Physiol. 275 (1998) L818–L826.
[51] L. Tacchini, L. Radice, A. Bernelli-Zazzera, J. Cell. Physiol. 180 (1999) 255–262.
[52] N. Golenhofen, R.B. Doctor, R. Bacallao, L.J. Mandel, Kidney Int. 48 (1995) 1837–1845.
[53] S.L. Ashworth, R.M. Sandoval, M. Hosford, J.R. Bamburg, B.A. Molitoris, Am. J. Physiol. 280 (2001) F886–F894.
[54] H. Shinohara, A. Tanaka, T. Fujimoto, E. Hatano, S. Satoh, K. Fujimoto, T. Noda, C. Ide, Y. Yamaoka, Biochim. Biophys. Acta 1317 (1996) 27–35.
[55] P.C. Dagher, Am. J. Physiol. 279 (2000) C1270–C1277.
[56] M. Hino, K. Kurogi, M.A. Okubo, M. Maruta-Hori, H. Hosoya, Biochem. Biophys. Res. Commun. 271 (2000) 164–169.
[57] C. Garnier, P. Barbier, R. Gilli, C. Lopez, V. Peyrot, C. Briand, Biochem. Biophys. Res. Commun. 250 (1998) 414–419.
[58] K. Morita, H. Wakui, A. Komatsuda, H. Ohtani, A.B. Miura, H. Itoh, Y. Tashima, Ren. Fail. 17 (1995) 405–419.
[59] E. Schiebel, Curr. Opin. Cell Biol. 12 (2000) 113–118.
[60] S. Gopalakrishan, N. Raman, S. Atkinson, J.A. Marrs, Am. J. Physiol. 275 (1998) C798–C809.
[61] S. Kawamura, S. Miyamoto, J.H. Brown, J. Biol. Chem. 278 (2003) 31111–31117.
[62] I.N. Fleming, C.M. Elliott, J.H. Exton, J. Biol. Chem. 271 (1996) 33067–33073.
[63] R.T. Watson, S. Shigematsu, S.H. Chiang, S. Mora, M. Kanzali, I.G. Macara, A.R. Saltiel, J.E. Pessin, J. Cell Biol. 154 (2001) 829–840.
[64] I.A. Prior, A. Harding, J.Y.J. Sluimer, R.G. Parton, J.F. Hancock, Nat. Cell Biol. 3 (2001) 368–375.
[65] G. Fritz, R. Gnad, B. Kaina, Anticancer Res. 19 (1999) 1681–1688.
[66] T. Trapp, L. Olah, I. Holker, M. Besselmann, C. Tiesler, K. Maeda, K.A. Hossmann, Mol. Cell. Neurosci. 17 (2001) 883–894.
[67] N. Granger, R.J. Korthuis, Annu. Rev. Physiol. 57 (1995) 311–332.
[68] M. Ozaki, S.S. Deshpande, P. Angkeow, S. Suzuki, K. Irani, J. Biol. Chem. 275 (2000) 35377–35383.
[69] K.-S Kim, K. Takeeda, R. Sethi, J.B. Pracyk, K. Tanaka, Y.F. Zhou, Z.-Y. Yu, V.J. Ferrans, J.T. Bruder, I. Kovesdi, K. Irani, P. Goldschmidt-Clermont, T. Kinkel, J. Clin. Invest. 101 (1998) 1821–1826.
[70] T. Kondo, K. Takeuchi, Y. Doi, S. Yonemura, S. Nagata, S. Tsukita, J. Cell Biol. 139 (1997) 749–758.
[71] N. Yoshinaga-Ohara, A. Takahashi, T. Uchiyama, M. Sasada, Exp. Cell Res. 278 (2002) 112–122.
[72] M. De La Vega, J. Burda, M.V. Toledo Lobo, M. Salinas, J. Neurosci. Res. 69 (2002) 540–549.
[73] A. Deten, A. Holzl, M. Leicht, W. Barth, H.G. Zimmer, J. Mol. Cell. Cardiol. 33 (2001) 1191–1207.
[74] Y. Gasche, M. Fujimura, Y. Morita-Fujimura, J.C. Copin, M. Kawase, J. Massengale, P.H. Chan, J. Cereb. Blood Flow Metab. 19 (1999) 1020–1028.
[75] M.K. Siu, W.M. Lee, C.Y. Cheng, Endocrinology 144 (2003) 371–387.
[76] R.O. Stuart, A. Sun, M. Panichas, S.C. Hebert, B.M. Brenner, S.K. Nigam, J. Cell. Physiol. 159 (1994) 423–433.
[77] T. Tsukamoto, S.K. Nigam, J. Biol. Chem. 272 (1997) 16133–16139.